Study of the phase transitions in $SmNiO_3$

1999 J. Phys.: Condens. Matter 11 405

(http://iopscience.iop.org/0953-8984/11/2/007)

J. Phys.: Condens. Matter **11** (1999) 405–415. Printed in the UK PII: S0953-8984(99)95943-X

Study of the phase transitions in $SmNiO_3$

J Pérez-Cacho†, J Blasco†§, J García†, M Castro‡ and J Stankiewicz†

† Departamento de Física de la Materia Condensada e Instituto de Ciencia de Materiales de Aragón, Universidad de Zaragoza–Consejo Superior de Investigaciones Científicas, 50009 Zaragoza, Spain

‡ Departamento de Ciencia de Materiales e Instituto de Ciencia de Materiales de Aragón, Centro Politécnico Superior, Universidad de Zaragoza, 50015 Zaragoza, Spain

Received 14 July 1998, in final form 22 September 1998

Abstract. $SmNiO_3$ has been synthesized under high oxygen pressure from a precursor prepared by means of a sol–gel method. The material obtained is of single phase and has an orthorhombic crystal structure at room temperature. The magnetic, electrical and thermal properties have been measured over a wide temperature range. This compound exhibits a metal–insulator and a paramagnetic–antiferromagnetic transition at 400 K and at 220 K, respectively. The metal–insulator transition is of first order while the magnetic ordering is a second order transition as can be inferred from calorimetric measurements. In addition, we observe an anomaly in the resistivity near the Néel temperature indicating a change in the conduction mechanism at this temperature. Our results support local antiferromagnetic correlations above the Néel temperature for this compound.

1. Introduction

Materials that exhibit a metal–insulator (MI) transition have attracted the interest of both solid state and material science researchers [1]. The nickelates $RNiO_3$, where R is a rare-earth element, exhibit an MI transition that varies with the rare-earth size [2, 3]. Thus they offer an unique opportunity to study the relationship between structural and electronic properties. It is well known that these oxides have distorted structures arising from the cubic perovskite structure [3]. The unit cell distortion as well as the Ni–O–Ni bond angle are related to the rare-earth ionic size. The least distorted one $LaNiO_3$, which has a rhombohedral unit cell, is a paramagnetic metal down to 1.5 K [4]. Other members of the $RNiO_3$ series (R = Pr, Nd, Sm, Eu) show the orthorhombically distorted structure of $GdFeO_3$ [5]. All of them exhibit an MI transition whose temperature increases, as the rare-earth size decreases, from 130 K (R = Pr) to 440 K (R = Eu) [2, 3]. In the insulating phase and at low temperatures, $RNiO_3$ exhibits rather complex antiferromagnetic ordering. It can be described by a commensurate $k = (1/2, 0, 1/2)$ spin density wave [6] which implies the presence of ferro- and antiferromagnetic interactions. Such a type of ordering can be explained by the formation of an orbital superlattice [7]. Both electronic localization and magnetic ordering occur at the same temperature in $PrNiO_3$ and $NdNiO_3$. The MI transition temperature is higher than the magnetic transition temperature for R = Sm and Eu.

In an earlier paper, we reported properties of $NdNiO_3$ that exhibits a first order MI transition at temperature $T_{MI} = 190$ K [8]. We have found that the entropy content associated with

§ Corresponding author: Javier Blasco. E-mail address: jbc@posta.unizar.es.

0953-8984/99/020405+11$19.50

the transition is lower than the expected one for a magnetic ordering of the spin $S = 1/2$ (Ni^{3+}) which occurs at the same temperature. Consequently, we have proposed that magnetic correlations must exist in $NdNiO_3$ at temperatures higher than T_{MI}. A strong enhancement of the effective mass of carriers, found from electrical and magnetic measurements, supports this conclusion. However, the coincidence of magnetic and MI transitions in $NdNiO_3$ obscures the interpretation of experimental results. In $SmNiO_3$, the MI transition takes place at $T_{MI} = 400$ K while magnetic ordering develops at 220 K. Therefore, both transitions can be studied independently.

We present here results of electrical, magnetic and thermal studies of $SmNiO_3$. Crystal structure and magnetic properties of the $SmScO_3$, that has been synthesized in order to understand the magnetic behaviour of the Sm^{3+} ion in a similar crystal structure, are also reported.

2. Experiment

$SmNiO_3$ has been obtained by means of a citrate route and thermal treatment under an oxygen pressure of 200 bars. Stoichiometric amounts of Sm_2O_3 and $2NiCO_3 \cdot 3Ni(OH)_2 \cdot 4H_2O$ were dissolved in nitric acid. After addition of citric acid and ethylene glycol in the appropriate ratio [9], the solution was heated until a green gel was formed. The gel was dried to obtain a brown powder which was calcined overnight at 500 °C in an oxygen current flow. The resulting black powder was pressed at 5 kbar into a bar-shaped sample and sintered at 1000 °C for 12 h under oxygen pressure of 200 bar.

$SmScO_3$ was prepared by standard ceramic procedures. Stoichiometric amounts of Sc_2O_3 and Sm_2O_3 were mixed, pelletized and calcined at 1250 °C in air for 3 days with intermediate regrindings.

The samples were checked by means of the x-ray diffraction technique and the patterns were of single phases. We note the high reproducibility of the synthetic procedure since different preparations have given samples with identical lattice parameters.

The chemical content of the $SmNiO_3$ was tested by fluorescence analysis using a JEOL JSM-6400 electronic microscope and a Link Analytical EDS x-ray spectrometer. Several sample parts of 1–2 μm^3 size were analysed. In all samples, the Sm:Ni atomic ratio agreed with the expected value within the experimental error. The oxygen content was determined by thermogravimetric analysis (TGA) in a reducing flow of N_2:H_2 (93:7). The samples show a slight oxygen deficiency and the nominal composition is $SmNiO_{2.96\pm0.02}$.

X-ray patterns were collected at room temperature for profile analysis in the 2θ range 18°–140° in steps of 0.02°. The counting rate was 8 s/step and a Rigaku D-max system working at 40 kV and 100 mA was used. A graphite monochromator coupled to the goniometer enables us to select the Cu $K\alpha_{1,2}$ radiation. The Rietveld analysis was made by using the Fullprof package program [10] and a pseudo-Voigt function was selected as the diffraction peak shape function.

Magnetic measurements were performed between 1.8 and 700 K in a commercial Quantum Design (SQUID) magnetometer and with a vibrating sample magnetometer. Resistance measurement was carried out using the standard six-probe dc method from 5 up to 550 K. Calorimetric measurements were done with an ac calorimeter (ACCI-VL Sinku-Riko) in the temperature range from 5 to 250 K and with a differential scanning calorimeter (DSC-7, Perkin–Elmer) up to 500 K. Additionally, the DSC measurements were used to scale the relative heat-capacity values obtained from ac calorimetry. Thermal expansion was measured between 150 and 500 K by using a push rod and differential transformer method.

3. Results and discussion

$SmNiO_3$ crystallizes in an orthorhombic $GdFeO_3$-type structure as has been reported earlier [5, 7]. However, we have not found any reference about the $SmScO_3$ structure. Its diffraction pattern is well described by an orthorhombic unit cell with *Pbnm* spatial group, similar to that of $SmNiO_3$. Such structure has been found for other scandium compounds such as $NdScO_3$ or $GdScO_3$ [11]. It can be viewed as a matrix of corner-shared MO_6 (M = Ni or Sc) octahedra; in it, Sm atoms are surrounded by eight octahedra. These octahedra can tilt (due to the small size of the Sm^{3+} ion) giving rise to the orthorhombic unit cell instead of the ideal cubic structure of a perovskite compound. Structural parameters, obtained from the Rietveld refinement of x-ray patterns, are given in table 1 for both compounds. The unit cell volume of $SmScO_3$ is larger than of $SmNiO_3$ as can be expected from the ionic size differences between Sc^{3+} and Ni^{3+}. This is also seen in the average interatomic distance between oxygen and the transition metal which is 2.095 Å for Sc–O and 1.955 Å for Ni–O. The Sc–O distance in $SmScO_3$ is equal to the calculated one with Sc^{3+} (0.745 Å) and O^{2-} (1.35 Å) ionic radii [12]. However, the Ni–O distance in $SmNiO_3$ is larger than the expected one for the Ni^{3+} low spin state (0.56 Å). It can be ascribed to the unit cell expansion of $SmNiO_3$ observed at the MI transition [13], which occurs well above room temperature [2].

Table 1. Unit cell parameters, fractional coordinates, reliability factors defined as in [10] and representative interatomic distances and angles for MO_6 octahedra (M = Ni, Sc) and Sm environment (eight-coordinated) in $SmNiO_3$ and $SmScO_3$. Structural refinements have been performed in the *Pbnm* spatial group, atoms are located as follows: M at (4b): (1/2, 0, 0); Sm and O(1) at (4c): (x, y, 1/4); O(2) at (8d): (x, y, z).

Sample		$SmNiO_3$	$SmScO_3$
a (Å)		5.3282(1)	5.5359(1)
b (Å)		5.4299(1)	5.7625(1)
c (Å)		7.5652(1)	7.9691(2)
V (Å^3)		218.87	254.22
Sm	x	0.9907(1)	0.9851(2)
	y	0.0511(1)	0.0563(1)
O(1)	x	0.087(1)	0.112(2)
	y	0.486(1)	0.458(1)
O(2)	x	0.708(1)	0.695(1)
	y	0.296(1)	0.302(1)
	z	0.042(1)	0.057(1)
B (Å^2)		0.12(3)	0.24(3)
R_{wp}	(%)	10.6	10.3
R_{Bragg}	(%)	4.1	4.9
χ^2		5.7	3.7
M–O(1) (Å)	2×	1.950(2)	2.100(4)
M–O(2) (Å)	2×	1.977(5)	2.101(4)
	2×	1.937(5)	2.085(4)
⟨M–O⟩ (Å)		1.959	2.095
M–O(1)–M (°)	2×	152.4(6)	143.1(2)
M–O(2)–M (°)	4×	151.9(10)	145.3(4)
⟨M–O–M⟩ (°)		152.6	144.6(4)
⟨Sm–O⟩$_8$ (Å)		2.469	2.543

The values of interatomic distances in table 1 show that the ScO_6 octahedra are nearly perfect at room temperature. Small differences in distance between Ni and the two equatorial

plane oxygen atoms appear in $SmNiO_3$ as has been observed in related nickelates [5]. We note that this slight distortion is larger for $SmNiO_3$ than for $NdNiO_3$ or $PrNiO_3$. Similar distortions observed in related manganese oxides have been ascribed to the presence of a Jahn–Teller effect [14]. Ni^{3+} is also a Jahn-Teller ion with a single electron in an orbitally degenerated ground state ($t_{2g}^6 e_g^1$). However, the anisotropy of the six Ni–O distances is very small and it can be a consequence of the more covalent character of the Ni oxides [15]. Furthermore, the distortion of the NiO_6 octahedra increases with decreasing rare earth size though the amount of Jahn–Teller ions (Ni^{3+}) remains unaltered. This points to the steric effect produced by the mismatch of the rare earth sizes as responsible for the NiO_6 distortion. In fact, similar behaviour is reported for perovskites without Jahn–Teller ions [16]. This feature can be understood within the frame of the bond valence model [17]. The increase of the NiO_6 distortion, when the rare earth size decreases, may be a consequence of higher electronegativity of smaller rare earth ions. The Ni^{3+} ion keeps its valence state by inducing a slight deformation of the NiO_6 octahedron. Similar results have been found for $EuNiO_3$ [18].

The Sm^{3+} ion size in $SmNiO_3$ and $SmScO_3$ is too small to assure that the MO_6 octahedra will not tilt. The effective oxygen coordination for Sm^{3+} is lower than in the ideal cubic structure (12). It is basically eight coordinated considering a cut-off of 3 Å in the Sm–O distances. Therefore, a similar crystal field splitting of the Sm^{3+} multiplet can be expected in both compounds. This facilitates the extraction of the magnetic contribution of the Ni^{3+} ions in $SmNiO_3$ as described below.

The most striking property of $SmNiO_3$ is the MI transition that occurs at 400 K. Figure 1 shows how the resistivity varies with temperature in $SmNiO_3$ samples. The resistivity jumps by three orders of magnitude at the transition point. This jump is accompanied by thermal hysteresis, indicating a first order transition. We note that the temperature range (≈20 K), in which thermal hysteresis in $SmNiO_3$ is observed, is smaller than the corresponding one in $NdNiO_3$ or $PrNiO_3$, where MI and magnetic ordering occur simultaneously. Above T_{MI}, the resistivity changes linearly with temperature as $\rho = \rho_0 + A_{e-ph}T$. This behaviour is typical for electron–phonon scattering. We obtain $\rho_0 = 4.6 \times 10^{-4}$ Ω cm, and $A_{e-ph} = 2.7 \times 10^{-6}$ Ω cm K^{-1} for $450 < T < 600$ K. These values are close to the ones found for

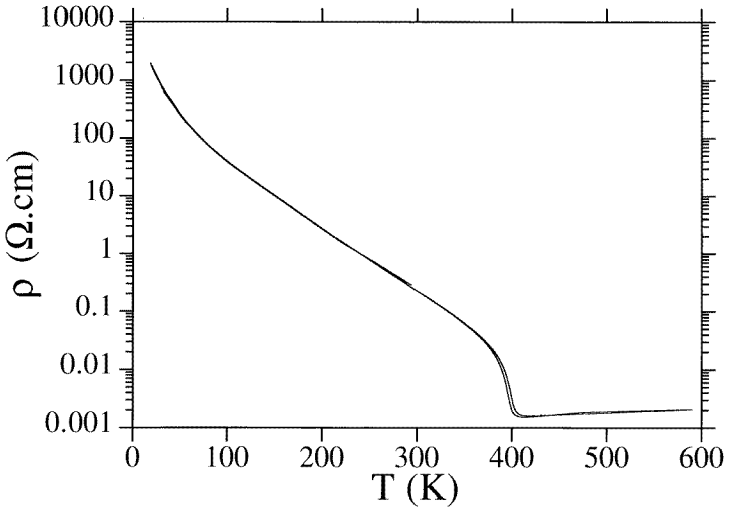

Figure 1. Resistivity against temperature for $SmNiO_3$.

related nickelates [4, 19]. Below T_{MI}, the resistivity shows a semiconducting-like behaviour but does not follow a simple energy activation model.

A $\ln\rho$ versus $1/T$ plot is shown in figure 2. The Arrhenius law is not followed in any temperature range. The resistivity exhibits a small anomaly at 220 K, that is more clearly seen in the $\mathrm{d}(\ln\rho)/\mathrm{d}T$ versus T plot shown in the inset of figure 2. This feature may be ascribed to the magnetic ordering developed below the same temperature (T_N), and may indicate a change in the electronic processes when the system is magnetically ordered. However, no such features are observed at T_N in other transition metal oxides which order antiferromagnetically [20]. On the other hand, similar step-like anomalies in ρ are observed at the charge-ordering temperature in some manganese oxides [21]. As the charge ordering is coupled to orbital ordering in several manganites [22], we might attribute the observed anomaly to the appearance of an orbital ordering in $SmNiO_3$ [7]. However, any reliable interpretation of our data requires Hall effect measurements as a function of T in order to separate carrier concentration and carrier mobility contributions to the conductivity. At the moment, we do not have these data.

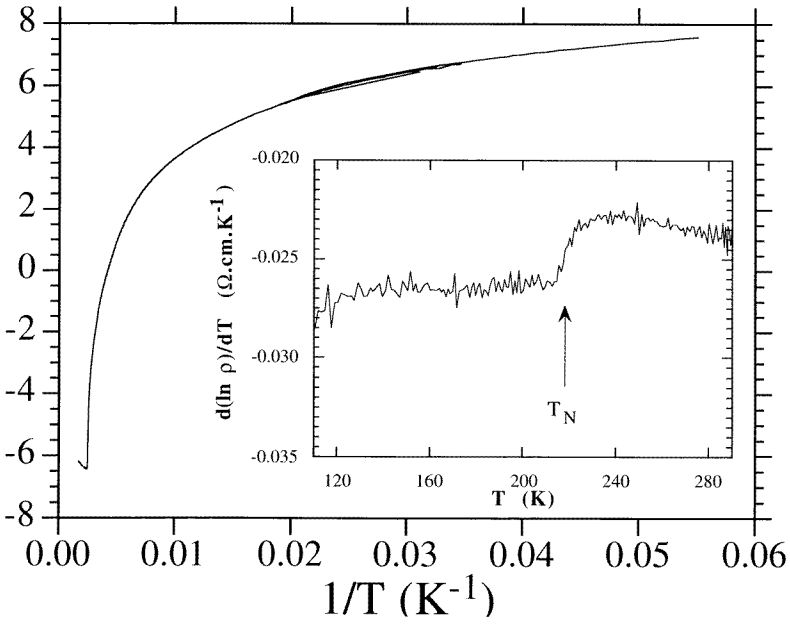

Figure 2. Neperian logarithm of the resistivity against $1/T$. The data were taken on cooling from 600 K down to 10 K. The inset shows the derivative $\mathrm{d}(\ln\rho)/\mathrm{d}T$ against T around the magnetic transition.

Figure 3 shows the dc susceptibility versus temperature curves for $SmNiO_3$ and $SmScO_3$. The susceptibility of $SmNiO_3$ exhibits a small kink around 220 K that corresponds to the magnetic arrangement of Ni^{3+}, in agreement with neutron diffraction data [13]. A strong rise in the paramagnetic signal at very low temperatures comes from the Sm^{3+} ions since both compounds, $SmScO_3$ and $SmNiO_3$, show the same behaviour. In addition, $SmNiO_3$ shows a maximum close to 2 K (see inset of figure 3) indicating the onset of long-range magnetic ordering in the Sm^{3+} sublattice. Long-range magnetic order of the rare-earth sublattice has been observed in several RMO_3 oxides (M = transition metal) at this low temperature range and the critical temperature depends on the strength of the R–M magnetic interaction [23]. The sample of $SmScO_3$ shows a minimum in the paramagnetic signal around 475 K arising from changes

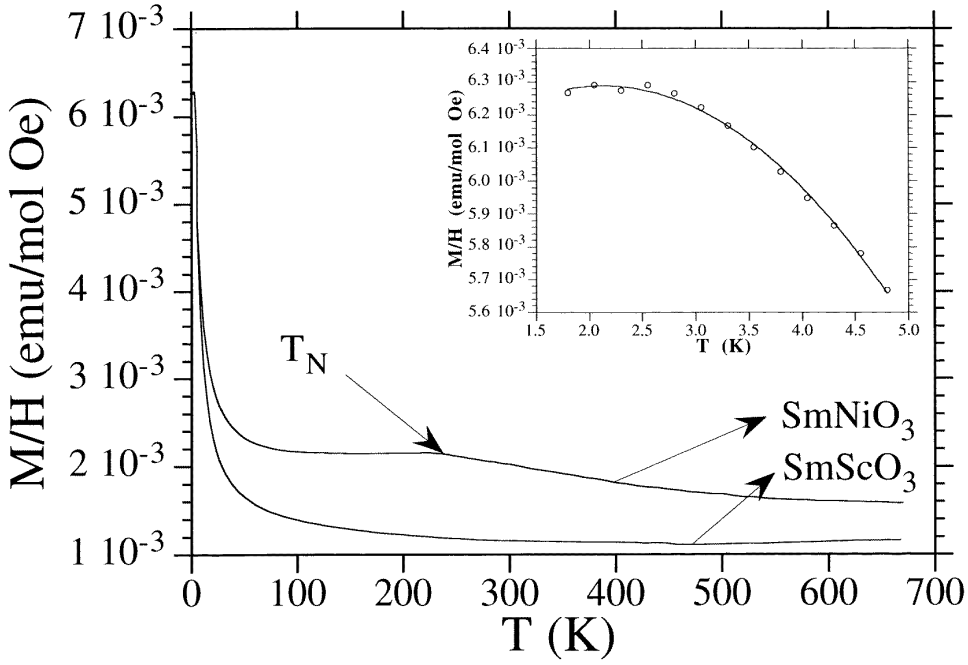

Figure 3. Dc susceptibility against temperature for $SmNiO_3$ and $SmScO_3$. The antiferromagnetic transition temperature for $SmNiO_3$ is indicated by an arrow in the figure. Inset: magnetic measurement for $SmNiO_3$ between 1.8 and 5 K. The line is a guide for the eye.

in the thermal population of the Sm^{3+} ion levels. Therefore, Sm^{3+} does not follow a Curie–Weiss law. In order to obtain the Ni^{3+} sublattice contribution to the magnetic susceptibility, we have subtracted the magnetic signal of $SmScO_3$ from the signal of $SmNiO_3$. The result is shown in figure 4. The susceptibility peaks at 220 K, which is the reported Néel temperature for $SmNiO_3$ [5, 7, 13]. Below T_N, the paramagnetic signal decreases down to $2/3$ of the cusp signal as is expected for a long-range antiferromagnetic ordering. The magnetic behaviour does not follow a Curie–Weiss law at high temperatures, as shown in the inset of figure 4. This can be attributed to magnetic interactions above T_N as is inferred from the calorimetric measurements (see below). A rough approximation of effective magnetic moments can be obtained from the fit of experimental data to the Curie–Weiss law between 280 and 400 K (insulating regime) and between 420 and 640 K (metallic regime). The values obtained are given in table 2. The effective magnetic moment increases as the temperature decreases. This feature has been also observed in manganese oxides with the same crystalline structure [24]. It has been attributed to the formation of ferromagnetic clusters in the paramagnetic state. We cannot discard the presence of magnetic clusters in the paramagnetic phase but it is difficult to judge their nature. In fact, the magnetic structure below T_N shows both ferro- and antiferromagnetic interactions. Attempts to detect small ferromagnetic clusters [25] by means of neutron diffraction at low angle (SANS) have been unsuccessful. Therefore, the formation of small antiferromagnetic clusters with spins not completely compensated is more likely. Surprisingly, the value of effective magnetic moments in the insulating regime agrees well with the one expected for a Ni^{3+} free ion (1.76 μ_B). The smaller value of the magnetic moment, obtained in the metallic phase, can be attributed to the electronic delocalization. Correspondingly, small values of effective magnetic moments have been found in metallic $NdNiO_3$ [9].

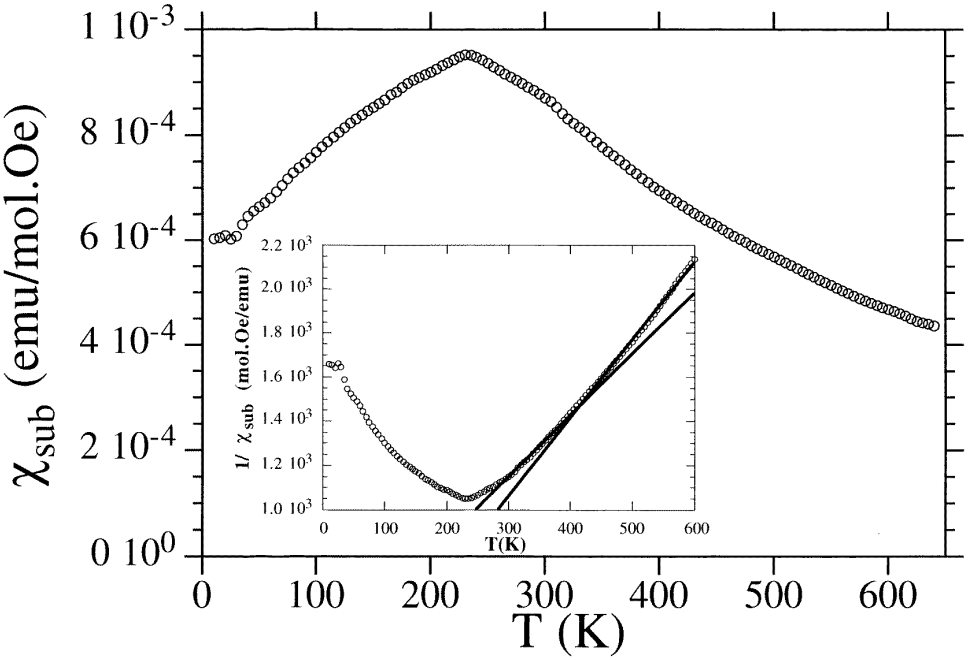

Figure 4. χ_{sub} against T. χ_{sub} is defined as $\chi(SmNiO_3) - \chi(SmScO_3)$. Inset: $1/\chi_{sub}$ against T; the lines are fits to the Curie–Weiss law in two temperature ranges.

Table 2. Magnetic parameters and calculated effective moments for $SmNiO_3$ obtained from the fit of the dc susceptibility to the Curie–Weiss law: $\chi = C/(T - \theta)$.

	280–400 K	420–640 K
C (emu K mol^{-1})	0.359	0.283(1)
θ (K)	−113	−1
μ_{eff} (μ_B fu^{-1})	1.69	1.50

The heat capacity of $SmNiO_3$ between 5 and 300 K is shown in figure 5. At low temperatures, the heat capacity exhibits a sharp increase indicating the beginning of an extra contribution in this range. Such behaviour can be ascribed to the onset of long range magnetic order in the Sm^{3+} sublattice (see inset of figure 3). At higher temperatures, a clear anomaly is detected at 220 K corresponding to the magnetic ordering of the Ni^{3+} ions. Anomalies at this temperature have also been observed in magnetic and transport measurements. Heat capacity data obtained upon heating and on cooling at a low rate of 5 K h^{-1} do not show a hysteretical behaviour through this transition. Therefore, a second order transition is suggested. In addition, the phase shift (ϕ) between the temperature oscillations induced in the sample and the heating power can indicate qualitatively the occurrence of a first order transition [26]. ϕ passes through a smooth and broad minimum at 220 K in $SmNiO_3$ (see inset (a), figure 5). This minimum is opposite in direction to the heat capacity anomaly, indicating the absence of a latent heat at transition. This supports a second order character of the transition. A first order transition implies that ϕ shows a peak and abrupt changes, in accordance with the heat capacity anomaly at the transition temperature, whose width gives the temperature range where two

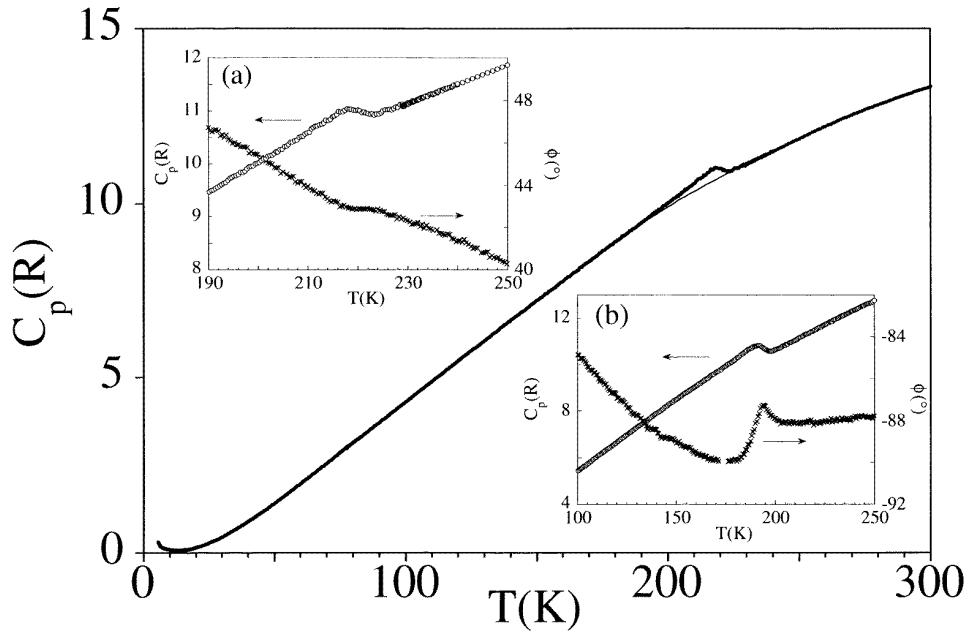

Figure 5. Heat capacity of $SmNiO_3$ against T (points); the solid line indicates the non-magnetic heat capacity obtained from the effective Debye temperature. Inset (a) details of the heat capacity and ϕ against T for $SmNiO_3$; ϕ is the phase shift between the temperature oscillations induced in the sample and the heating power. Inset (b) heat capacity and ϕ against T for $NdNiO_3$.

thermodynamic phases exist. Such behaviour has been observed in the $NdNiO_3$ compound [8, 9]. A clear peak in the phase shift was detected for this compound at 190 K (see inset (b), figure 5), and a range of 12 K of two-phase coexistence was determined from the peak width when the measurements were done at 30 K h^{-1}. $NdNiO_3$ develops first order MI and magnetic transitions simultaneously. The present study shows that the magnetic transition in $SmNiO_3$ is second order transition.

In order to estimate the entropy content corresponding to the magnetic transition in $SmNiO_3$, information on non-magnetic heat capacity contributions is necessary. It has been calculated by an interpolation method using the effective Debye temperature which varies smoothly with temperature and allow us an easy interpolation. The excess heat capacity (the difference between the total measured value and the non-magnetic contribution) is represented in figure 6. The peak obtained has a maximum of about 0.4 R and the calculated entropy variation between 180 and 230 K is $\Delta S = 0.03\ R$. This value is much lower than the theoretical value for the magnetic ordering of Ni^{3+} ($S = 1/2$) ions ($\Delta S = R \ln 2 = 0.69\ R$) and is also smaller than ΔS found for $NdNiO_3$ (0.12 R) measured by ac calorimetry [8, 9]. As discussed above, magnetic and MI transitions occur at the same temperature in $NdNiO_3$ and, consequently, both transitions contribute to the entropy content. In $SmNiO_3$, these transitions are separate. In order to obtain accurate values of entropies and enthalpies through the MI transition we performed DSC measurements in both compounds. The values obtained, with scans of 20 °C min^{-1}, for the MI transition at 404 K in $SmNiO_3$ are $\Delta H = 650$ J mol^{-1} and $\Delta S = 0.2\ R$. The same measurement performed on $NdNiO_3$ gives $\Delta H = 315$ J mol^{-1} and $\Delta S = 0.2\ R$ at 194 K. The difference between the entropies determined by DSC and ac calorimetry is due to the fact that with ac calorimetry we measured the heat capacity directly

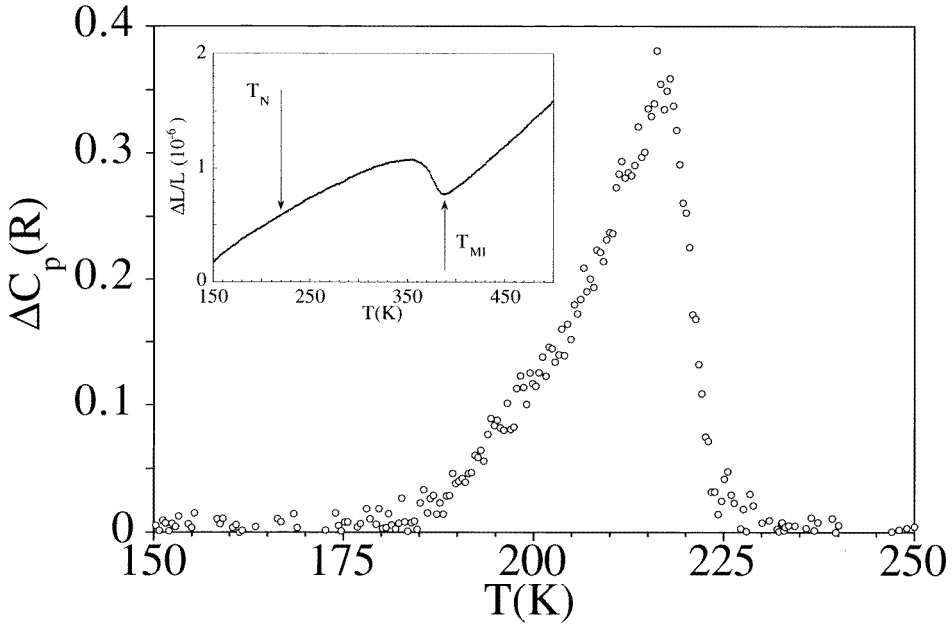

Figure 6. The excess heat capacity against T near the magnetic transition. Inset: linear thermal expansion against T for $SmNiO_3$.

and not the enthalpy. Then, the entropy content due to discontinuous enthalpy changes cannot be determined. In addition, the study of the maximum temperature variation (DSC peak) with the heat-flow rate (from 2°C min^{-1} up to 20 °C min^{-1}) has been done on heating and on cooling. The Sm compound shows a small hysteresis of 1.2 K, within the experimental error, while in the Nd compound the hysteresis is 26 K wide, in agreement with the resistivity measurements.

Linear thermal expansion measurements for $SmNiO_3$ are shown in the inset of figure 6. $\Delta L/L$ shows a jump at the MI transition which corresponds to an expansion in the volume of 0.1% with decreasing temperature. This result is in agreement with the one obtained from neutron diffraction experiments [7, 13]. No anomaly is observed at the magnetic transition as can be inferred from the inset of figure 6. The metallic phase shows a linear thermal expansion with a dilatation coefficient of 7.8×10^{-6} K^{-1}. Otherwise, the thermal expansion curve is bent below T_{MI} and the average dilatation coefficient is 4.6×10^{-6} K^{-1}.

The MI transitions in the nickelates have been explained by a competition between two characteristic energies: the conduction bandwidth, W, and the charge transfer energy, Δ [3]. W depends strongly on the Ni–O–Ni bond angle that controls the electronic transfer between Ni 3d and O 2p atomic orbitals. The large orthorhombic distortion observed in $SmNiO_3$, i.e., small values of Ni–O–Ni angle (see table 1), implies a high T_{MI}. The volume change at the T_{MI}, detected by several techniques [9, 13], supports this claim. This change is related to the small increase of the Ni–O–Ni angle through the transition and $W > \Delta$ above T_{MI} while $W < \Delta$ below T_{MI}. More difficult is to establish what drives the MI transition in the nickelates studied. A gap of magnetic origin seems unlikely, since T_N and T_{MI} differ substantially in $SmNiO_3$. Another possibility is an orbital ordering, as detected in related systems [22], that is established at T_N for $NdNiO_3$ and $PrNiO_3$ or above T_N for

$SmNiO_3$ and $EuNiO_3$. Such ordering is supported by the type of magnetic ordering observed in these compounds at low temperature [6, 7]. Furthermore, the antiferromagnetic structure is explained by the Ni e_g orbital ordering which gives rise to ferro- and antiferromagnetic interactions between neighbouring atoms depending on which orbital is occupied for each atom. Our x-ray diffraction measurements with high counting rate show no evidence of such orbital ordering in the $SmNiO_3$ at room temperature (insulating paramagnetic phase). These results are in agreement with recent neutron diffraction studies [7] although the presence of such orbital ordering cannot be discarded. In addition, our resistivity results seem to indicate that a long range orbital ordering would occur at T_N, much below the MI transition temperature. Finally, the formation of small polaron formation in the insulating phase, as has been previously suggested [27], can provide another explanation. It is clear from our results that antiferromagnetic correlations exist above T_N in these oxides. This is indicated by the nearly null entropy change (as compared to the one expected for magnetic ordering of Ni^{3+} ions) shown by the magnetic transition in both $SmNiO_3$ and $NdNiO_3$. Therefore, the formation of spin polarons with antiferromagnetic correlations seems to be plausible as has been suggested for $NdNi_{1-x}Cu_xO_3$ [8], and it seems to be a general feature in this kind of nickelates. We suggest that local antiferromagnetic correlations give rise to an electronic localization at high temperatures in $SmNiO_3$ and, as temperature decreases, a long-range antiferromagnetic ordering is developed. This ordering is also reflected by a small anomaly in the resistivity curve that indicates a change in the conduction mechanism. Further work on the frequency dependence of the ac resistivity is needed in order to establish the role, if any, of antiferromagnetic polarons.

4. Conclusions

The nickelate $SmNiO_3$ synthesized at high oxygen pressure has been studied by means of dc magnetic susceptibility, dc resistivity, linear thermal expansion and ac calorimetry. A linear dependence of the electrical resistivity on temperature in the metallic phase is found. Electron–phonon scattering is responsible for such behaviour. In the insulating phase, the electrical conduction does not follow a thermal activation mechanism but the activation energy decreases with decreasing temperature. An anomaly in the resistivity has been detected for the first time at T_N indicating a change in the conduction mechanism when the system orders antiferromagnetically. Calorimetric studies suggest the existence of antiferromagnetic correlations in the paramagnetic phase. The very low entropy change for the magnetic transition in $SmNiO_3$ and $NdNiO_3$ is not well understood yet. The existence of spin polarons with high effective mass and local antiferromagnetic correlations can account for such behaviour. In addition, we report for the first time the crystal structure for the $SmScO_3$.

Acknowledgment

We thank DGICYT for financial support (project Nos MAT96-0491 and MAT97-0987).

References

[1] Goodenough J B 1971 *Prog. Solid State Chem.* **5** 276
[2] Lacorre P, Torrance J B, Pannetier J, Nazzal A I, Wang P W and Huang T C 1991 *J. Solid State Chem.* **91** 225
[3] Torrance J B, Lacorre P, Nazzal A I, Ansaldo E J and Niedermayer Ch 1992 *Phys. Rev.* B **45** R8209
[4] Rajeev K P, Shivashankar G V and Raychaudhuri A K 1991 *Solid State Commun.* **7** 591
[5] García-Muñoz J L, Rodríguez-Carvajal J, Lacorre P and Torrance J B 1992 *Phys. Rev.* B **46** 4414

[6] García-Muñoz J L, Rodríguez-Carvajal J and Lacorre P 1992 *Europhys. Lett.* **20** 241
[7] Rodríguez-Carvajal J, Rosenkranz S, Medarde M, Lacorre P, Fernändez-Díaz M T, Fauth F and Trounov V 1998 *Phys. Rev.* B **57** 456
[8] Pérez J, Stankiewicz J, Blasco J, Castro M and García J 1996 *J. Phys.: Condens. Matter* **8** 10 393
[9] Blasco J, Castro M and García J 1994 *J. Phys.: Condens. Matter* **6** 5875
[10] Rodríguez-Carvajal J 1993 *Physica* B **192** 55
[11] Geller S 1957 *Acta Crystallogr.* **10** 243
[12] Shannon R D 1976 *Acta Crystallogr.* A **32** 751
[13] García-Muñoz J L, Rodríguez-Carvajal J and Lacorre P 1994 *Phys. Rev.* B **50** 978
[14] Radaelli P G, Cox D E, Marezio M, Cheong S-W, Schiffer P E and Ramirez A P 1995 *Phys. Rev. Lett.* **75** 4488
[15] García J, Blasco J, Proietti M G and Benfatto M 1995 *Phys. Rev.* B **52** 15 823
[16] Liu X and Prewit C T 1991 *J. Phys. Chem. Solids* **52** 441
[17] Brown I D and Shannon R D 1973 *Acta Crystallogr.* A **29** 266
[18] Alonso J A, Martínez-Lope M J and Rasines I 1995 *J. Solid State Chem.* **120** 170
[19] Granados X, Fontcuberta J, Obradors X, Mañosa Ll and Torrance J B 1993 *Phys. Rev.* B **48** 11 666
[20] Briático J, Alascio B, Allub R, Butera A, Caneiro A, Causa M T and Tovar M 1996 *Phys. Rev.* B **53** 14 020
[21] Ibarra M R, De Teresa J M, Blasco J, Algarabel P A, Marquina C, García J, Stankiewicz J and Ritter C 1997 *Phys. Rev.* B **56** 8252
[22] Murakami Y, Kawada H, Kawata H, Tanaka M, Arima T, Moritomo Y and Tokura Y 1998 *Phys. Rev. Lett.* **80** 1932
[23] Bartolomé F, Kuz'min M D, Bartolomé J, Blasco J, García J and Sapiña F 1994 *Solid State Commun.* **91** 177
[24] Goodenough J B 1997 *J. Alloys Compounds* **262/263** 1
[25] De Teresa J M, Ibarra M R, Algarabel P A, Ritter C, Marquina C, Blasco J, García J, del Moral A and Arnold Z 1997 *Nature* **386** 256
[26] Garland C W 1985 *Therm. Acta* **88** 127
Castro M and Puértolas J A 1997 *Therm. Acta* **304/305** 291
[27] Goodenough J B, Mott N F, Pouchard M, Demazeau G and Hagenmuller P 1973 *Mater. Res. Bull.* **8** 647